# Properties of Mixed Species/Densities Cross Laminated Timber made of Rubberwood and Coconut Wood

Suthon Srivaro[1,2,3]*, Hyungsuk Lim[4], Minghao Li[5], Zoltan Pasztory[6]

[1]Center of Excellence in Wood and Biomaterials, Walailak University, Thasala district, Nakhon Si Thammarat 80160, Thailand

[2]School of Engineering and Technology, Walailak University, Thasala district, Nakhon Si Thammarat 80160, Thailand

[3]Center of Excellence on Petrochemical and Materials Technology, Chulalongkorn University, Soi Chula 12, Phayathai Road, Pathumwan, Bangkok, 10330, Thailand

[4]School of Forestry, University of Canterbury, Private Bag 4800, Christchurch, New Zealand

[5]Department of Civil and Natural Resources Engineering, University of Canterbury, Private Bag 4800, Christchurch 8140, New Zealand

[6]Innovation Center, University of Sopron, Hungary

**Abstract**

The utilization of rubberwood (*Hevea brasiliensis*) and coconut wood (*Cocos nucifera L.*), the essential economic crops in Thailand and tropical countries, was proposed for manufacturing mixed species/density cross-laminated timber (CLT) for building construction. Six 3-layer CLT configurations, which are composed of either medium-density (600 – 799 $kg/m^3$) rubberwood (MRB) or coconut wood (MCC) or high-density (800 – 999 $kg/m^3$) coconut wood (HCC) laminations, were determined considering the mechanical properties and material costs. The outer layers of the control MCC CLT were replaced with either MRB or HCC to improve its mechanical properties, while either outer or core layers of the control MRB CLT were replaced with HCC to reduce its material cost. The material properties of the three wood types and the six CLT configurations were examined. The densities of the produced CLTs were not affected by the chosen manufacturing parameters showing a strong correlation to the lamination's density. From the bonding performance perspective, the mixed-species approach significantly increased the average wood failure percentage of the control MRB CLT. However, only the control MCC CLT achieved the average wood failure percentage greater than 80%, as required in North America's CLT standard. The compressive strength properties of the CLTs in their major strength directions, $\sigma_{clt}$, were governed by the outer laminations' parallel-to-grain compressive strength. Unlike softwood CLTs, neglecting the load sharing contribution of the core layer in the $\sigma_{clt}$ estimation resulted in 15% underestimation. Rolling shear strength, $\tau_{rs}$, was determined by the core laminations regardless of the CLT layups. MRB achieved the highest $\tau_{rs}$ followed by HCC and MCC, and all values were significantly larger than the common softwood used in CLT production. The results imply that the mixed species/densities approaches can effectively improve the mechanical properties of the coconut wood CLT and reduce the material cost of rubberwood CLT without compromising structural performance.

**Keywords:** Cross laminated timber, rubberwood, coconut wood, mixed species, mixed densities

## 1. Introduction

Since cross laminated timber (CLT) was first introduced in Europe around the 1990s, it has gained more popularity for mid to high rise building construction [1-3]. This trend has been reflected in an increasing number of buildings constructed with CLT worldwide, such as 18-storey Mjøstårnet building (Brumunddal, Norway), 18- storey Brock Commons Tallwood House (Vancouver, Canada), and 10-storey Forte building (Melbourne, Australia). Several researchers around the world have studied the feasibility of manufacturing CLT using various wood species [4-10].

Recently, many attempts have been made to develop hybrid (or mixed- species) CLT partly due to the limited wood resources [11-19]. One advantage of combing different wood species is to utilize low-grade wood in CLT while still meeting the structural requirement. The mixed-species CLT can be made out of softwood and hardwood, different hardwood or softwood species. Moreover, engineered wood composites, such as oriented strand board (OSB), laminated veneer lumber (LVL), and plywood, have also been used for producing hybrid CLT to expand their use in mid to high-rise building construction [20-27].

As by-products from plantation crops in tropical countries, rubberwood (*Hevea brasiliensis)* and coconut wood (*Cocos nucifera L.*) can be potentially used for CLT production due to their reasonably good mechanical properties [28-29]. Previously, rubberwood has been used for glued laminated timber production [30] while coconut wood is used as rafter and beam [31]. Recently, CLT specimens using a single species of rubberwood or coconut wood have been successfully manufactured [9-10,15, 32]. Besides the mechanical properties, the raw material cost also affects the CLT production cost. In Thailand, manufacturers determine the rubberwood and coconut wood prices, which vary on their production scales, marketing strategies, and locations. Rubberwood logs are typically processed in sawmills equipped with band headrigs and carriages to fresh-sawn lumber and dried at rubberwood factories using conventional drying kilns. On the other hand, coconut tree plantation owners or local sellers process coconut logs into lumber on small scales using chain or circular saws at the plantation area. The fresh-sawn coconut lumber is then air-dried and transported to the local markets. Based on the communication with the rubberwood industry in Nakhon Si Thammarat province, Thailand, the average selling price of the rubberwood (˜550 USD/cu.m.) is approximately twice as expensive as coconut wood (Goldgeer 58 Co., Ltd; Khaomahachai Parawood CO., LTD., Nakhon Si Thammarat Province, Thailand). In addition, the price and properties of coconut wood also vary with its density. Higher density coconut wood is stronger but more expensive than lower density coconut wood [29, 31].

Thus, mixed-species CLT production using rubberwood and coconut wood was proposed considering Thailand's material availability and cost-efficiency. The basic physical and mechanical properties of the rubberwood and coconut wood laminations with medium (600 – 799 kg/m$^3$) and high (800 – 999 kg/m$^3$) densities were measured. Then, the rubber-coconut CLT lay-ups were determined to improve the medium-density coconut wood CLT's material properties and reduce the raw material cost of the rubberwood CLT. The physical and mechanical properties of the rubber-coconut CLT specimens, along with their bonding performance, were examined and compared with those of the single wood species/density CLTs.

## 2. Materials and Methods

### 2.1 Preparation and property tests of wood raw materials

The kiln-dried rubberwood lumber with the dimensions of 80 mm (width) × 20 mm (thick) × 1,000 mm (length) were randomly selected from a local factory in Nakhon Si

Thammarat province, Thailand. Thus, the annual ring orientation of the lumber was not controlled. Only lumber free of natural defects such as knot and pith was chosen for CLT production. The lumber pieces were processed to dimensions of 75 mm (width) × 15 mm (thick) × 300 mm (length) and then conditioned at 20 °C and relative humidity of 65% for about two months. The average density and moisture content of the rubberwood at the time of CLT production were 706±34 kg/m$^3$ and 12.3±0.6%, respectively.

The coconut wood lumber was prepared from 40-year old coconut trees planted in Thalassa district, Nakhon Si Thammarat province, Thailand. The coconut trunks were flat sawn to obtain the lumber dimensions of 100 mm (width) × 25 mm (thick) × 1,000 mm (length). The lumber pieces were dried with a laboratory drying kiln at dry-bulb and wet-bulb temperatures of 60 °C and 45 °C, respectively, for about two weeks. Subsequently, the pieces were processed to dimensions of 75 mm (width) × 15 mm (thick) × 300 mm (length). Then, they were conditioned at 20 °C and relative humidity of 65% for about two months. The average moisture content of the conditioned coconut wood was 13.2±1.3%.

The basic material properties of the conditioned wood samples were measured: density, modulus of rupture (MOR), modulus of elasticity (MOE), and compressive strength parallel to the grain, $\sigma_{c\|}$, were measured. The densities of the conditioned samples were measured according to ASTM D2395 [33], and they were grouped into two density groups: medium and high. The density ranged from 614 to 782 kg/m$^3$ and 805 to 951 kg/m$^3$ for the medium- and high-density groups, respectively. For simplicity, the medium- and high-density coconut wood groups are denoted MCC and HCC, respectively, while rubberwood is denoted MRB. For each group, 10 bending and 10 compression tests were conducted following ASTM D143 [34] with modified specimen dimensions. Bending MOR and MOE were determined by center point bending tests using a span to thickness ratio of 14 (see Figure 1a). The dimensions of the bending test specimens were 15 mm (thick) × 25 mm (width) × 240 mm (length). The MOE measured by implementing the described test setup would be approximately 90% of the true MOE [35]. The dimensions of the compression parallel to the grain test specimens were 15 mm (thick) × 22 mm (width) × 30 mm (length) (See Figure 1b). A loading rate of 2 mm/min was used for both bending and compression tests. MOR, MOE, and $\sigma_{c\parallel}$ were calculated by using the equations 1, 2, and 3 respectively.

$$MOR = \frac{3P_{max}L}{2bh^2} \tag{1}$$

$$MOE = \frac{L^3}{4bh^3}\left(\frac{P}{\Delta}\right) \tag{2}$$

$$\sigma_{c\parallel} = \frac{F_{C-max}}{A_c} \tag{3}$$

where $P_{max}$ is the maximum bending load, L is the loading span length, b is the width of a test specimen, h is the height of a test specimen, P/Δ is the slope of a load-deflection curve within an elastic range, $F_{C\text{-}max}$ is the maximum compressive load, and $A_c$ is the cross-sectional area of a specimen.

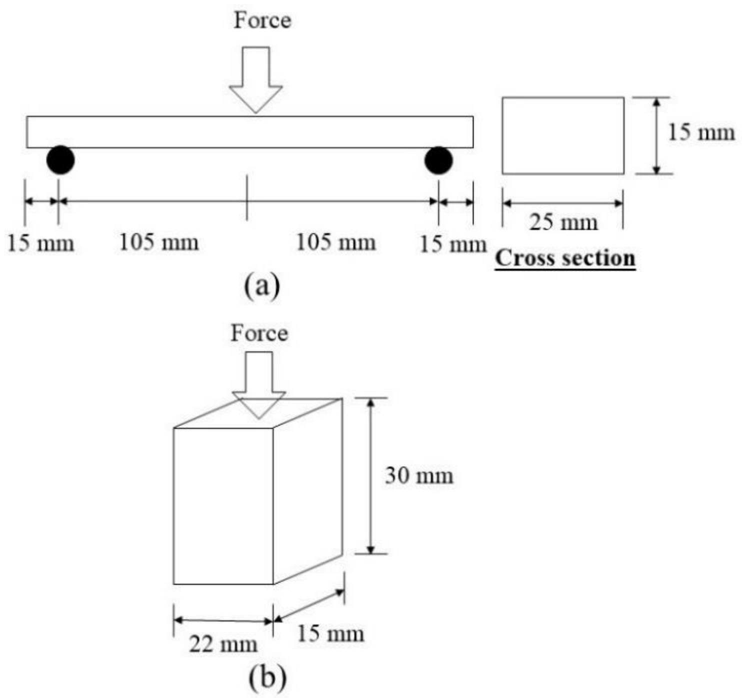


**Figure 1** Schematic drawings of (a) three-point bending and (b) compression in parallel direction to the grain tests.

## 2.2 Manufacturing and property tests of cross laminated timber

Three-layer cross laminated timber (CLT) panels with the dimensions of 300 mm (width) × 300 mm (length) × 45 mm (thickness) were manufactured. In total, six CLT configurations were manufactured (see Figure 2). The CLT configurations made of a single wood species with the medium density described earlier were used as the control groups. Considering the number and order of layers, they are denoted MRB-MRB-MRB and MCC-MCC-MCC. Mixed-species/densities CLT configurations were then designed to improve the mechanical properties of MCC-MCC-MCC and reduce the manufacturing cost of MRB-MRB-MRB. Based on the obtained compressive strength parallel to the grain (HCC>MRB=MCC, see Table 2) and modulus of elasticity (HCC>MRB>MCC, see Table 2), the surface layers of the control MCC group was replaced with either HCC or MRB laminations. These mixed-species/densities CLT configurations were denoted HCC-MCC-HCC and MRB-MCC-MRB. In contrast the surface and core layers of the control MRB group were replaced with HCC laminations considering the cost of original wood materials (MRB>HCC), which were denoted HCC-MRB-HCC and MRB-HCC-MRB, respectively. However, MCC laminations were not chosen as potential substitutes to avoid the compensation of the control MRB group's mechanical properties.

For each configuration, three CLT panels, which make eighteen in total, were manufactured in two steps. First, four laminations of the same species and density range were edge-glued with polyvinyl acetate to form a single panel with the dimensions of 300 mm (width) × 300 mm (length) × 15 mm (thickness). A mechanical clamp was used to consolidate the lamination edges with the glue applied at a rate of 100 $g/m^2$ [10]. The single-layered panels were clamped for 20 min, and then their faces were sanded with 120 grits to remove the excess glue and be activated for bonding. In the second step, three single-layered panels were face-glued into CLT panels using one-component polyurethane. The glue was applied to one of the two bonding faces at a rate of 300 g/m$^2$ [10, 32], and then the assembled CLT panels were pressed under a clamping pressure of 2.45 MPa (pressure gauge) for 120 min. The CLT panels were cut to the material property test specimens, as described in Table 1, which were conditioned at 20 °C and relative humidity of 65% for about two weeks before the tests.

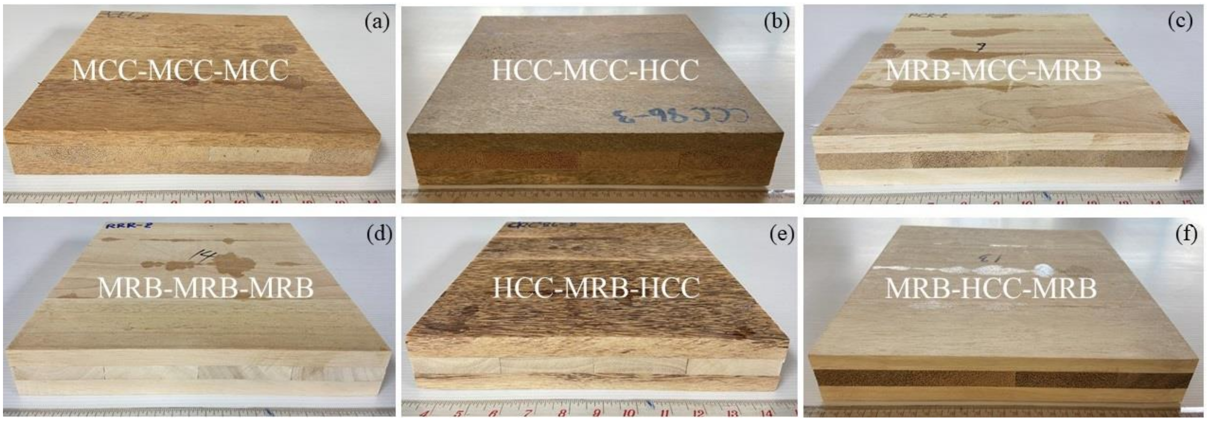


**Figure 2** Photos of six CLT panels with different lay-ups.

**Table 1** Dimensions and numbers of material property test specimens

| Test type | Dimensions (mm) | | | No. (/config.) |
|---|---|---|---|---|
| | L | W | T | |
| Density | 40 | 40 | 45 | 15 |
| Bonding (block shear) | 45 | 40 | 30 | 12 |
| Compression | 40 | 40 | 45 | 12 |
| Short-span bending (rolling shear) | 290 | 50 | 45 | 10 |

Note: L, W, and T are in major, minor, and thickness-wise directions, respectively.

The density was measured following ASTM D2395 [33] to evaluate the effect of clamping pressure on it. Block shear tests were conducted according to ASTM D905 [36] to measure the bonding strength and wood failure percentage. Stair-step test specimens were prepared, as illustrated in Figure 3, which were loaded on their surface laminations in parallel to their fiber directions until the bonded areas were sheared away. The bonding shear strength, $\tau_{bond}$, was calculated using the following equation

$$\tau_{bond} = \frac{V_{max}}{A_{bond}} \quad (4)$$

where $V_{max}$ is the maximum shear load of a test specimen and $A_{bond}$ is the bonding area of a test specimen. The images of tested planes were recorded and analyzed using image processing software (MultiSpecWin64 (free-ware), Purdue University, USA) to determine wood failure percentages.

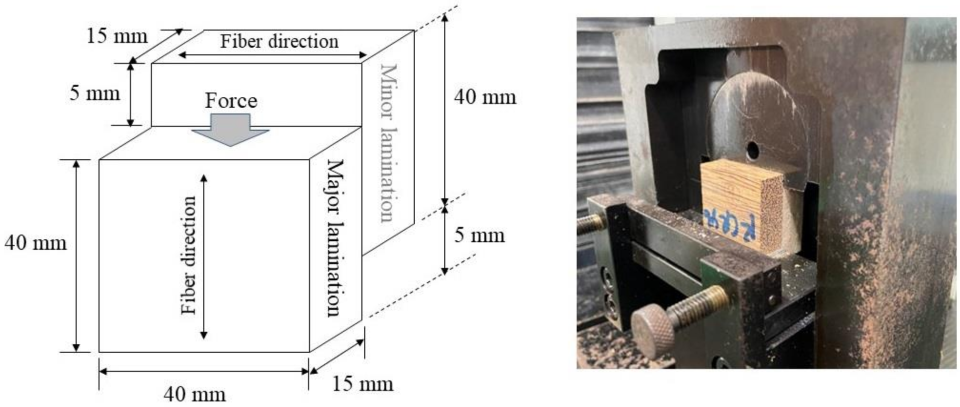


(a) (b)

**Figure 3** (a) Schematic drawing of block shear test specimen and (b) Experimental figure for block shear test.

Compression tests were conducted in the CLT's major strength direction (i.e. parallel to the fiber direction of the surface laminations) to evaluate the influence of cross- or core-laminations on the compressive strength, $\sigma_{clt}$, of the mixed-species/densities CLTs. $\sigma_{clt}$ was calculated using the following equation

$$\sigma_{clt} = \frac{F_{clt\_max}}{A_{clt}} \quad (5)$$

where $F_{clt\_max}$ is the maximum compressive load applied to a CLT specimen, and $A_{clt}$ is the loaded cross-sectional area of a CLT specimen.

The rolling shear strength, $\tau_{rs}$, of each CLT configuration was determined from short-span bending tests conducted at a span-to-depth ratio of 5. Thus, the loading span and the overhang from each specimen end were 225mm and 32.5mm, respectively. $\tau_{rs}$ was calculated according to the simplified method described in CLT handbook [1] using the following equations in order.

$$EI_{eff} = \sum_{i=1}^{n} E_i b_i \frac{h_i^{\,3}}{12} + \sum_{i=1}^{n} E_i A_i z_i^{\,2} \tag{6}$$

$$\left(\frac{Ib}{Q}\right)_{eff} = \frac{EI_{eff}}{\sum_{i=1}^{n/2} E_i h_i z_i} \tag{7}$$

$$\tau_{rs} = \frac{P_{maxo\_clt}}{2\left(\frac{Ib}{Q}\right)_{eff}} \tag{8}$$

where $P_{max\_clt}$ is the maximum bending load obtained from a short-span bending test, $E_i$ is Young's modulus of the i^th^ layer of a test specimen, $z_i$ is the distance from the center of the i^th^ layer to the center of the middle layer of a test specimen, and $b_i$ is the width of a test specimen. The Young's modulus of the cross-layer was assumed to be one-thirtieth of its longitudinal Young's modulus.

The compression and short-span bending tests were conducted using a universal testing machine (Lloy, UK) with a loading rate of 2 mm/min. The statistical difference between the mean values was analyzed by one-way ANOVA analysis at 0.05 level of significance.

## 3. Results and discussion

### 3.1 Properties of wood raw materials

The physical and mechanical properties of the rubberwood and coconut wood used in CLT production are shown in Table 2. At the medium density range (i.e. 600 – 799 kg/m$^3$), the compressive strength parallel to grain $\sigma_{c\parallel}$ of coconut wood (MCC) and rubberwood (MRB) were similar but the average MOR and MOE values of MCC were lower. This might be due to their different anatomical structures and cell wall characteristics. For coconut wood, the thin-walled parenchyma cell (foam-like cell) is surrounded by thick-walled fiber cell (honeycomb-like structure) to form wood tissues with a large variation of properties across its transverse section [29, 31, 37]. In contrast, rubberwood is composed of fibre cells with honeycomb-like structures throughout its transverse section [28,37]. Despite the described anatomical differences, the average MOE and $\sigma_{c\parallel}$ values of the high-density coconut wood (HCC) were significantly larger than those of MBR. Although the MOR of HCC was larger than MRB, the differences were not significant. Moreover, the test results confirm that the density of coconut wood determines its mechanical properties as reported in authors' previous work [29].

**Table 2** Properties of original rubberwood and coconut wood used in CLT production.

| Types of wood species | $\rho$ (kg/m$^3$) | MOR (MPa) | MOE (MPa) | $\sigma_{c\parallel}$ (MPa) |
|---|---|---|---|---|
| rubberwood (MRB) | 706±34$^b$ | 95.9±6.9$^a$ | 10,292±776$^b$ | 47.8±2.3$^b$ |
| coconut wood (MCC) | 713±44$^b$ | 85.1±8.3$^b$ | 8,293±824$^c$ | 48.0±2.6$^b$ |
| high-density coconut wood (HCC) | 870±61$^a$ | 104.5±12.0$^a$ | 11,167±560$^a$ | 63.9±11.3$^a$ |

***** Groups with the same superscript letters (a or b) in column indicate that the mean values are not significantly difference based on one-way ANOVA test at 0.05 level of significance.

## 3.2 Properties of CLT materials

### 3.2.1 Density

The average densities of MRB-MRB-MRB, HCC-MRB-HCC, MRB-HCC-MRB, MCC-MCC-MCC, HCC-MCC-HCC, and MRB-MCC-MRB configurations were 693±30 kg/m$^3$, 823±42 kg/m$^3$, 768±32 kg/m$^3$, 675±25 kg/m$^3$, 823±46 kg/m$^3$, and 697±26 kg/m$^3$, respectively. As shown in Figure 4, these measured values of the mixed-species/densities configurations had a strong linear relationship at an R-squared coefficient of 0.97 with the densities estimated using the rule of mixtures expressed in the following equation.

$$\rho_{CLT} = f_{outer}\rho_{outer} + (1 - f_{outer})\rho_{core} \tag{9}$$

where $f_{outer}$ is the volume-based fraction of outer layers, $\rho_{outer}$ and $\rho_{core}$ are the average densities of species used for the outer and core layers found in Table 2.

Thus, the chosen pressing parameters did not densify any CLT configurations and can be adopted for manufacturing them at larger scales depending on their bonding performance, described in the next section.

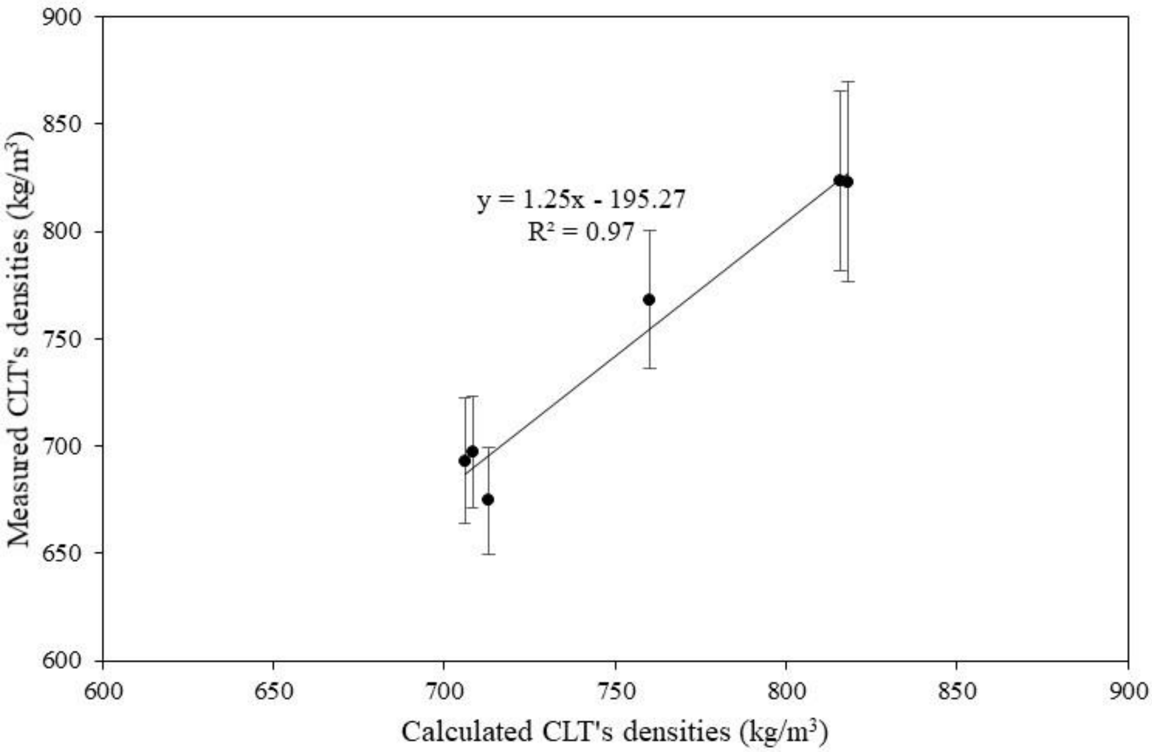


**Figure 4** Relationship between the measured and calculated densities by means of a rule of mixtures.

### 3.2.2 Bonding performance

The average bonding shear strength $\tau_{bond}$ of the six CLT configurations are shown in Figure 5, along with their standard deviations. The control MRB configuration's $\tau_{bond}$ was significantly higher than that of the control MCC configuration mainly due to the shear strength differences between the two species [28-29]. Replacing the surface layers of the control MCC configuration with either HCC or MRB laminations did not affect $\tau_{bond}$. Although MRB replacements with HCC reduced $\tau_{bond}$ of the control MRB configuration, the strength differences were not statistically significant.

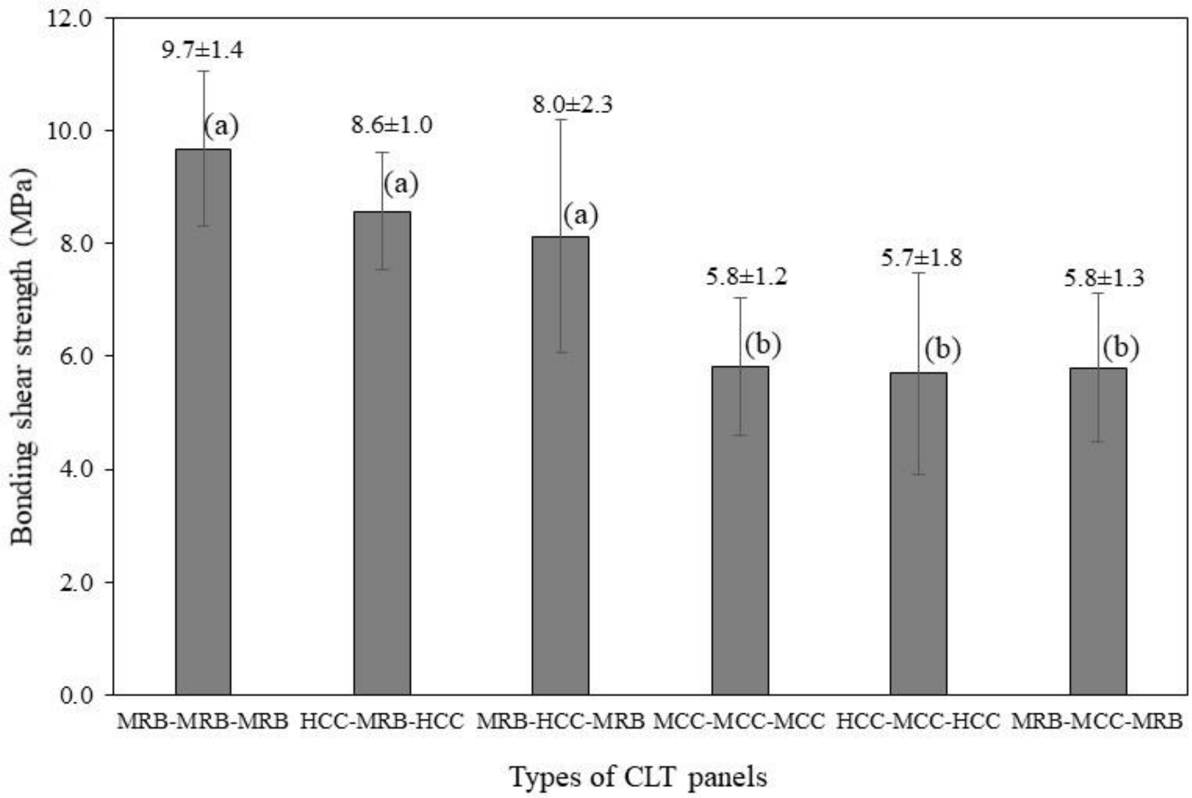


**Figure 5** Bonding shear strength of CLT specimens. Groups with the same letters (a or b) indicate that the mean values are not significantly difference based on one-way ANOVA test at 0.05 level of significance.

The laminations perpendicularly aligned to the loading direction were failed in shear for the MCC configurations (i.e. MCC-MCC-MCC, MRB-MCC-MRB, and HCC-MCC-HCC), as shown in Figure 6a. This observation confirms that the perpendicular-to-grain shear strength of the core laminations contributed more to the $\tau_{bond}$ than the parallel-to-grain shear strength of the outer laminations regardless of the lay-ups. In contrast, the MRB configurations had different governing failure modes depending on the lay-ups, as shown in Figure 6b. The control MRB specimens failed due to poor adhesive bonding, while the HCC laminations of the mixed MRB species failed in shear. Thus, the governing failure mode was changed from adhesive failure to parallel-to-grain and perpendicular-to-grain failures when the HCC laminations replaced the control MRB's surface layers (i.e. HCC-MRB-HCC) and core layers (i.e. MRB-HCC-MRB), respectively. These observations imply that the shear strength of HCC governed $\tau_{bond}$ of the two mixed MRB CLT lay-ups and may support that the perpendicular-to-grain shear strength of the MRB laminations would have been larger than the parallel-to-grain strength of the HCC laminations.

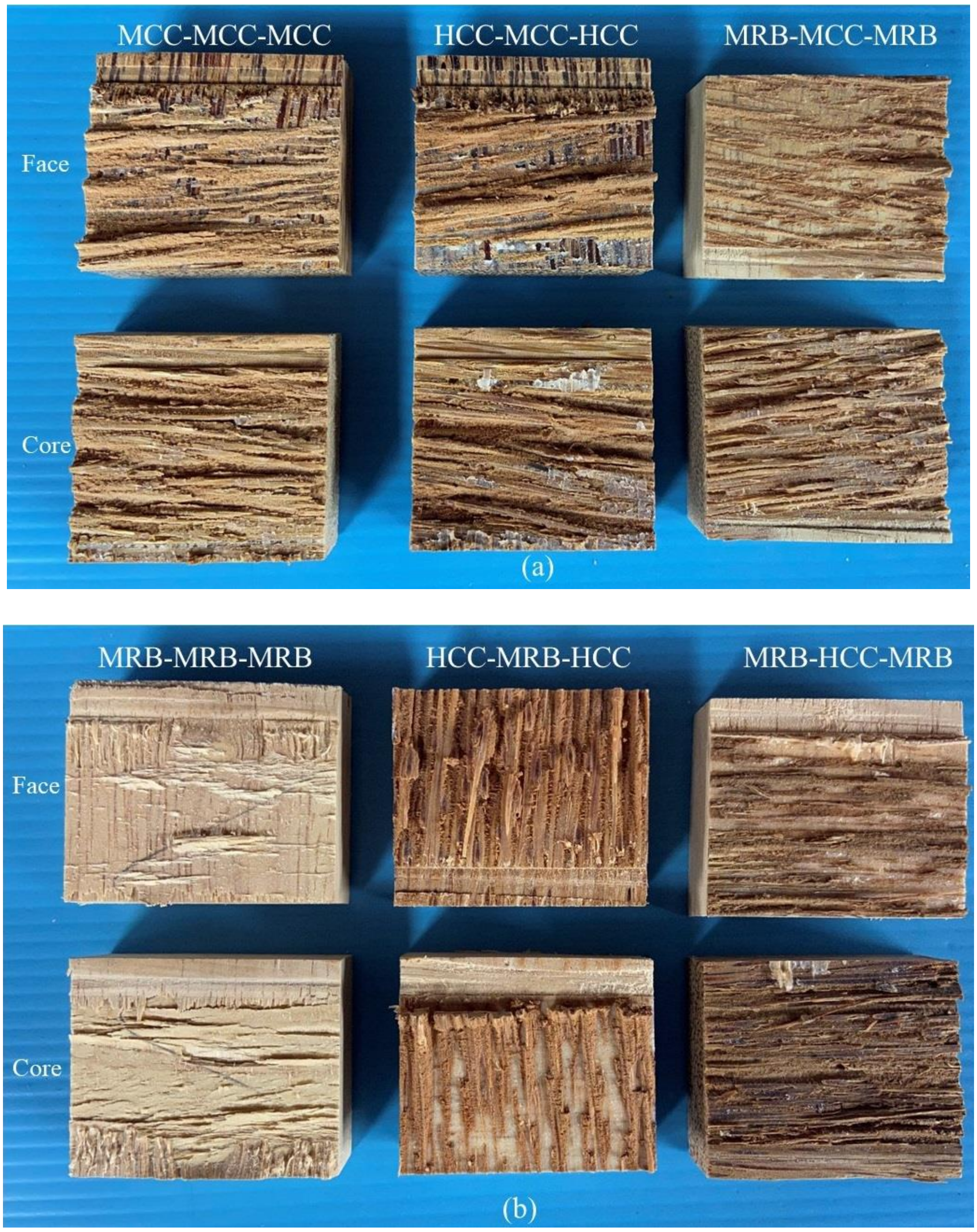


**Figure 6** Fracture surface of the specimen after block shear test (a) MCC-MCC-MCC, HCC-MCC-HCC, MRB-MCC-MRB and (b) MRB-MRB-MRB, HCC-MRB-HCC, MRB-HCC-MRB.

The average wood failure percentage (WFP) of the six CLT lay-ups are shown in Figure 7. WFP of the control MRB was 10±8 % which was significantly lower than that of the control

MCC (i.e. 86±24 %). Considering that the wood failures of the control MRB were relatively shallow compared to those of the control MCC, the polyurethane adhesive would have penetrated the coconut wood deeper than the rubberwood at the same density range, through its more porous structure composed of parenchyma cells. When the HCC laminations replaced either outer or core laminations of the control MRB, the average WFP increased to 54±26 % and 71±28 % for MRB-HCC-MRB and HCC-MRB-HCC, respectively. This observation implies that the anatomical structure of the higher-density coconut wood is more favorable for bonding than that of the lower-density rubberwood. Thus, the mixed-species manufacturing approach with coconut wood can be considered for improving the bonding performance of rubberwood CLT from the wood failure perspective. In contrast, the HCC and MRB replacements decreased the average WFP of the control MCC configuration. In addition to the anatomical structure difference between the two species described above, the lower fraction of parenchyma cells in HCC compared to MCC [29] explains this trend. However, among the six CLT configurations, only the control MCC met the minimum average WFP criteria (i.e. 80%) of the North America CLT product standard [1]. Thus, pressing parameter modifications and the use of more compatible adhesives are necessary to be studied in the future.

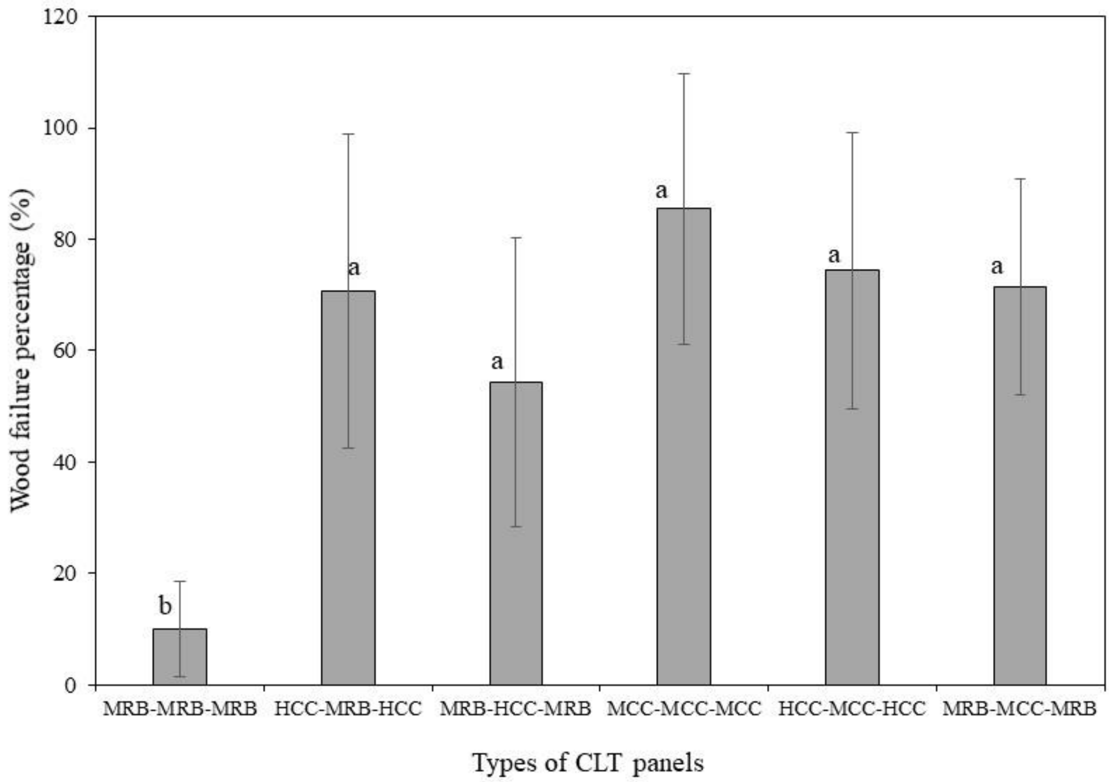


**Figure 7** Wood failure percentage of the shear plane area of test specimens after block shear test. Groups with the same letters (a or b) indicate that the mean values are not significantly difference based on one-way ANOVA test at 0.05 level of significance.

### 3.2.3 Compressive strength in major strength direction ($\sigma_{clt}$)

The average compressive strength in the major strength direction ($\sigma_{clt}$) of the produced CLT specimens are shown in Figure 8, with the bars indicating their standard deviations. The test results showed that the $\sigma_{c\parallel}$ of the outer laminations determined the $\sigma_{clt}$ values. Replacing the outer layers of the control MCC and MRB CLT lay-ups with the HCC laminations (i.e. HCC-MRB-HCC and HCC-MCC-HCC) improved the $\sigma_{clt}$ regardless of the core lamination materials. On the other hand, since the $\sigma_{c\parallel}$ properties of the MRB and MCC laminations were statistically similar, as presented in Table 2, the CLT configurations with either MRB or MCC outer laminations had statistically similar $\sigma_{clt}$ values. Thus, given the same density range, coconut wood can be considered over rubberwood for manufacturing CLTs for wall applications at a lower price without compromising vertical load resistance.

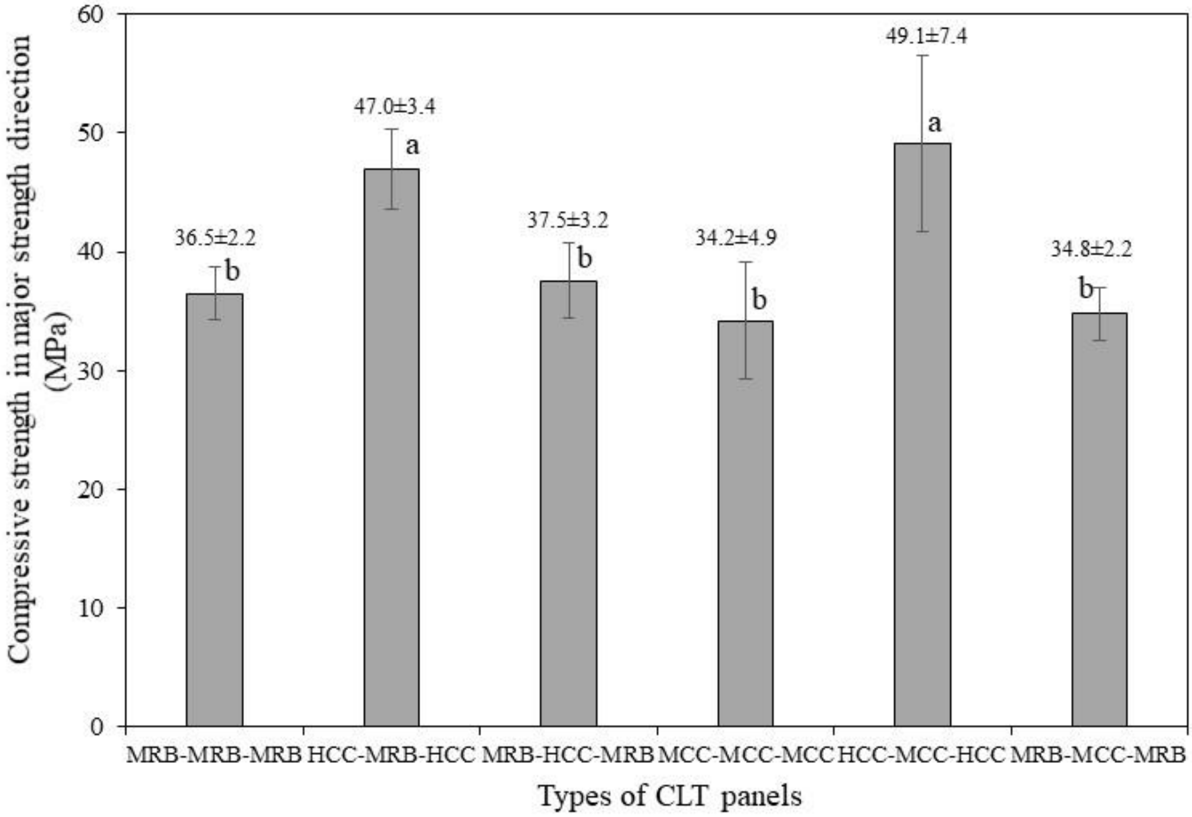


**Figure 8** Compressive strength in major strength direction of CLT specimens. Groups with the same letters (a or b) indicate that the mean values are not significantly difference based on one-way ANOVA test at 0.05 level of significance.

Based on the discussion above and as recommended in the CLT Handbook [1], the $\sigma_{clt}$ values could be estimated using the $\sigma_{c\parallel}$ of the laminations aligned parallel to the CLT's major axis. Thus, the estimated compressive strength in the major direction $\sigma_{clt\_est}$ of a three-layer CLT was calculated using the following equation.

$$\sigma_{clt\_est} = \frac{2A_{outer}\sigma_{c\parallel\_outer}}{A_{clt}} \tag{10}$$

where $A_{clt}$ is the total cross-sectional area of a CLT subjected to compression; $A_{outer}$ and $\sigma_{c\parallel\_outer}$ are the cross-sectional area and the $\sigma_{c\parallel}$ of one outer lamination (Table 2), respectively. Since the contribution of the core laminations on the $\sigma_{clt}$ was ignored, the $\sigma_{clt\_est}$ values were expected to be lower than the average measured values, as shown in Table 3, and used as design values [1]. Although the degree of underestimation varied among the six CLT configurations, it was large as 15% when the HCC laminations replaced the core layer of the control MRB CLT. Therefore, the assumption that the cross-laminations negligibly contribute to the $\sigma_{clt}$ needs to be validated for the CLTs produced with rubberwood or coconut wood or both through further research before it gets adopted for estimating $\sigma_{clt}$.

**Table 3** Estimated compressive strength properties of the six CLT configurations and their comparisons against the measured values.

| Configuration | $\sigma_{clt\_est}$ (MPa) | $\sigma_{clt\_est}$ /$\sigma_{clt}$ |
|---|---|---|
| MRB-MRB-MRB | 31.9 | 0.87 |
| HCC-MRB-HCC | 42.6 | 0.91 |
| MRB-HCC-MRB | 31.9 | 0.85 |
| MCC-MCC-MCC | 32.0 | 0.94 |
| HCC-MCC-HCC | 42.6 | 0.87 |
| MRB-MCC-MRB | 31.9 | 0.92 |

From the failure mode perspective, the outer laminations fractured under the compressive loads applied along the CLT major direction (Figure 9). Here, failure mechanisms observed in the rubberwood and coconut wood laminations were slightly different. In rubberwood, the failure was initially a result of crushing and folding of the wood cell in microscopic level like other hardwood species [38-39], consequently the failure band was obviously seen in macroscopic level as shown in Figure 8.  In coconut wood, however, a combination of crushing and longitudinal splitting of the wood cells were observed. Cracking initiated along the parenchyma cell due to its relatively low strength [31].


**Figure 9** Fracture of specimens after compression test.

Compared to the conventional softwood CLTs, such as Black spruce CLT three ply (35-35-35) (21.1 MPa, [40]) and Canadian Hemlock five (35-35-35-35-35) ply (26.1 MPa, [41]), the average compressive strength values of CLTs produced in this work (34.2-49.1 MPa) was approximately 1.3-2.3 times larger at a similar test scale. This implies that the produced CLTs would achieve the higher vertical load carrying capacity than softwood CLTs when it is used as a load-bearing wall. However, establishing of characteristic values for practical design of this CLT panel is still required to be done in future work.

### 3.2.4 Rolling shear strength ($\tau_{rs}$)

The average rolling shear strengths, $\tau_{rs}$, of the six CLT configurations are shown in Figure 10, along with their standard deviations. In 3-ply CLT, $\tau_{rs}$ is theoretically determined by its core layer and shall not be affected by its outer layers. Besides the core laminations' material properties, such as width-to-depth ratio, density, and defects, test and calculation methods affect the $\tau_{rs}$ measurements. At the medium density range, $\tau_{rs}$ of the rubberwood CLT was approximately 1.6 times higher than the coconut wood CLT. As expected, the average $\tau_{rs}$ values of the CLT configurations with the same core layer materials were statistically the same as shown in Figure 10. Although the differences were not statistically significant, the $\tau_{rs}$ of MCC obtained from the control MCC CLT specimens was 13% lower than those obtained by the HCC-MCC-HCC and MRB-MCC-MRB specimens. Given that the MOE of MCC was much lower than HCC and MRB, this observation implies that the bending stiffness of the outer laminations may have affected $\tau_{rs}$ measurements when the center-point short-span test is implemented along with simplified calculation method. Further research can validate this implication through experimental studies and numerical modeling work. On the other hand, the average $\tau_{rs}$ of the HCC laminations obtained from the MRB-HCC-MRB was significantly lower than that of the MRB laminations while generally larger than the $\tau_{rs}$ of MCC due to having more fiber cells [29].

Compared to the common softwood species, such as Southern pine ($\tau_{RS}$=1.77-1.89 MPa, [42]), Douglas fir ($\tau_{RS}$=1.35-2.51 MPa, [43]), Radiata pine ($\tau_{RS}$=1.67-2.45 MPa, [43]), and Black spruce ($\tau_{RS}$=1.73 MPa, [40]), used for CLT production, MRB ($\tau_{RS}$=6.2-6.4 MPa), MCC ($\tau_{RS}$=3.9-4.5 MPa), and HCC ($\tau_{RS}$=5.2 MPa) all reached approximately 1.6-4.7 times larger rolling shear capacities. Thus, the CLTs made of the proposed materials would be less restricted by the rolling shear strength in designing floor members subjected to short-span bending and punctual loading by vertical members. During construction, the higher rolling shear strength would also help prevent the shear failure of the areas around CLT panel lifting points [44].

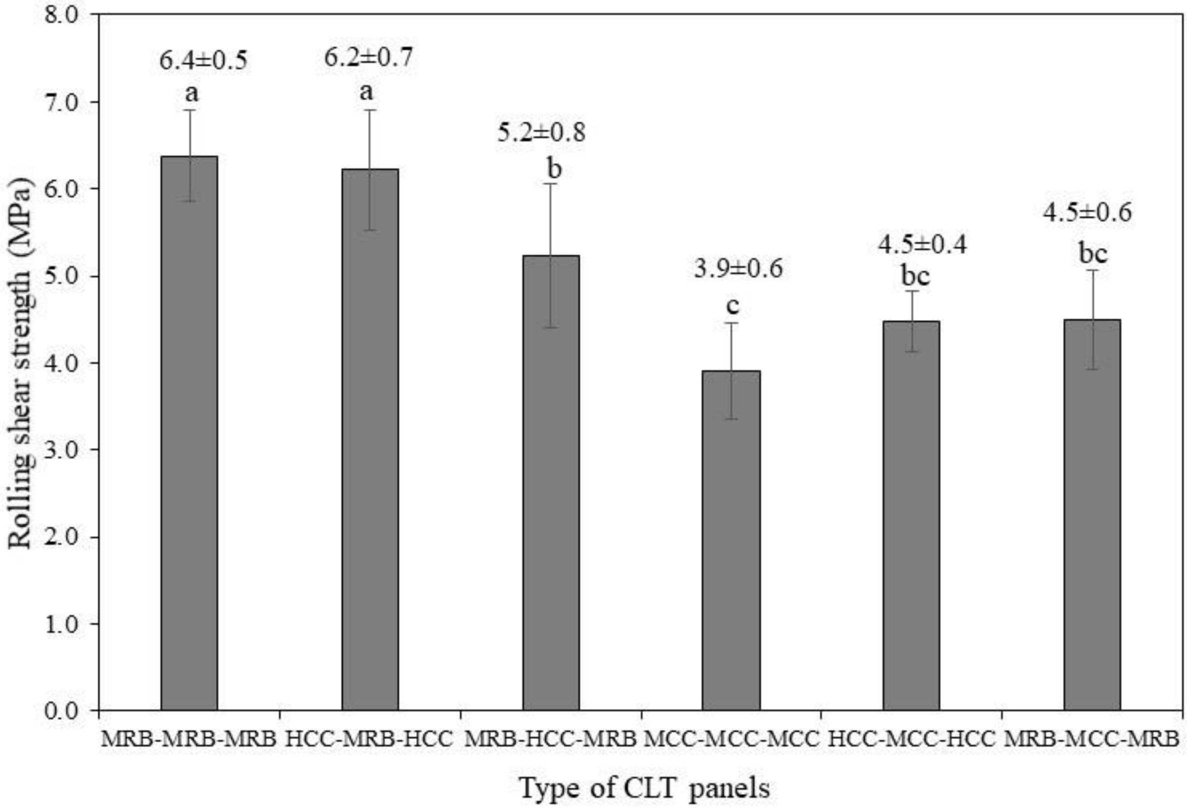


**Figure 10** Rolling shear strength of the produced CLT panels. Groups with the same letters (a or b) indicate that the mean values are not significantly difference based on one-way ANOVA test at 0.05 level of significance.

Figure 11 shows the typical rolling shear failures experienced by the six CLT configurations. Despite the differences in anatomical features between the utilized species and common softwood species [40,42-44], similar failure patterns were observed. Micro cracks formed at approximately 45° to the neutral axes of the test specimens, propagated towards the bond lines and caused either core or outer laminations to fracture along the bond lines. Figure 12 shows the typical crack formation occurred in the HCC, MCC, and MRB core laminations in details. Interestingly, the shear cracks formed in the coconut wood propagated through their parenchyma cells regardless of density. This observation indicates that the characteristics of parenchyma cells govern the $\tau_{rs}$ of coconut wood, and thus larger for higher-density coconut wood [45], as presented in Figure 10.

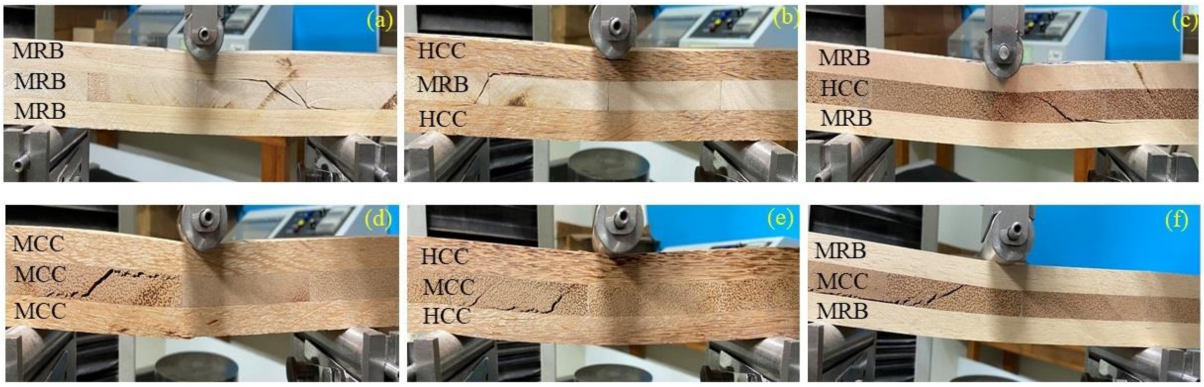


**Figure 11** Typical rolling shear failures of the produced mixed species CLT panels, (a) MRB-MRB-MRB, (b) HCC-MRB-HCC, (c) MRB-HCC-MRB, (d) MCC-MCC-MCC, (e) HCC-MCC-HCC and (f) MRB-MCC-MRB.

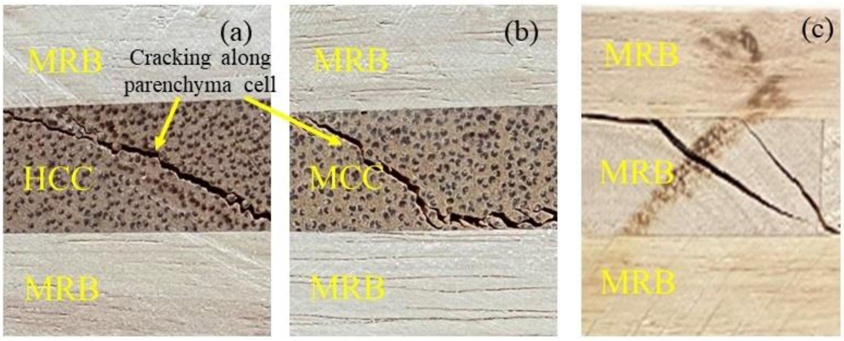


**Figure 12** Typical shear crack formation observed in the (a) MRB-HCC-MRB, (b) MRB-MCC-MRB and (c) MRB-MRB-MRB specimens.

## 4. Conclusions

In this study, mixed species/density CLT manufacturing approaches were implemented to improve mechanical properties of coconut wood CLT and reduce the material cost of rubberwood CLT without compromising structural performance. Based on the experimentally obtained material properties of the medium-density coconut wood (MCC), high-density coconut wood (HCC), and medium-density rubberwood (MRB), six CLT lay-ups, including two controls, were determined, manufactured, and destructively tested. The chosen pressing parameters did not densify any CLT configurations. The main findings are listed as follows:

- Although the mixed species approach improved the bonding performance of the control MRB CLT, the implemented consolidation process, including glue-application and pressing, did not provide satisfactory bonding to the CLT configurations, except the control MCC CLT. Therefore, further research on optimizing the consolidation process that guarantees bonding performance is needed.
- The outer laminations governed the compressive strength in the major direction of the CLT specimens; however, the contribution of the core laminations could not be neglected, unlike softwood CLTs.
- Rolling shear strength of MRB was significantly higher than HCC and MCC, which makes MRB an attractive choice for the core-laminations. Thus, the CLT lay-up with HCC outer and MRB core laminations would achieve the best mechanical properties.
- Furthermore, considering that the coconut wood's mechanical properties, including rolling shear strength, are better than or similar to common softwood, the mixed- or single-density coconut wood CLTs would achieve structural performance comparable to common softwood CLTs at significantly lower costs than the CLTs composed of rubberwood.

**Acknowledgement**

The authors would like to thank the financial support from the National Research Fund and Walailak University (Grant No. N42A650375). The support from University of Sopron, Hungary through the “Sustainable Raw Material Management Thematic Network – RING 2017”, EFOP-3.6.2-16-2017-00010 project in the framework of the Szechenyi 2020 Program which is supported by the European Union, co-financed by the European Social Fund is also acknowledged. Adhesives used in this work is supported by PJ Chonburi Parawood Co., Ltd., Chonburi, Thailand.

**References**

[1] FPInnovations. (2013). CLT Handbook, US Edition.

[2] Brandner, R., Flatscher, G., Ringhofer, A., Schickhofer, G., & Thiel, A. (2016). Cross laminated timber (CLT): overview and development. *European Journal of Wood and Wood Products*, 74(3), 331-351.

[3] Muszynski, L., Hansen, E., Fernando, S., Schwarzmann, G., & Rainer, J. (2017). Insights into the global cross-laminated timber industry. *BioProducts Business*, 77-92.

[4] Liao, Y., Tu, D., Zhou, J., Zhou, H., Yun, H., Gu, J., & Hu, C. (2017). Feasibility of manufacturing cross-laminated timber using fast-grown small diameter eucalyptus lumbers. *Construction and Building Materials, 132*, 508-515.

[5] Srivaro, S., Matan, N., & Lam, F. (2019). Performance of cross laminated timber made of oil palm trunk waste for building construction: a pilot study. *European Journal of Wood and Wood Products*, 77(3), 353-365.

[6] Yusof, N. M., Tahir, P. M., Lee, S. H., Khan, M. A., & James, R. M. S. (2019). Mechanical and physical properties of Cross-Laminated Timber made from Acacia mangium wood as function of adhesive types. *Journal of wood science*, *65*(1), 1-11.

[7] Gui, T., Cai, S., Wang, Z., & Zhou, J. (2020). Influence of Aspect Ratio on Rolling Shear Properties of Fast-Grown Small Diameter Eucalyptus Lumber. *Journal of Renewable Materials*, *8*(9), 1053-1066.

[8] Ma, Y., Musah, M., Si, R., Dai, Q., Xie, X., Wang, X., & Ross, R. J. (2021a). Integrated experimental and numerical study on flexural properties of cross laminated timber made of low-value sugar maple lumber. *Construction and Building Materials, 280*, 122508.

[9] Srivaro, S., Pásztory, Z., Le Duong, H. A., Lim, H., Jantawee, S., & Tomad, J. (2021a). Physical, mechanical and thermal properties of cross laminated timber made with coconut wood. *European Journal of Wood and Wood Products*, 79(6), 1519-1529.

[10] Srivaro, S., Leelatanon, S., Setkit, M., Matan, N., Khongtong, S., Jantawee, S., & Tomad, J. (2021b). Effects of manufacturing parameters on properties of rubberwood-cross laminated timber manufactured via hot pressing. *Journal of Building Engineering*, 44, 102703.

[11] Aicher, S., Hirsch, M., & Christian, Z. (2016). Hybrid cross-laminated timber plates with beech wood cross-layers. *Construction and Building Materials*, 124, 1007-1018.

[12] Kim, K. H. (2020). Influence of layer arrangement on bonding and bending performances of cross-laminated timber using two different species. *BioResources*, *15*(3), 5328-5341.

[13] Ma, Y., Si, R., Musah, M., Dai, Q., Xie, X., Wang, X., & Ross, R. J. (2021b). Mechanical Property Evaluation of Hybrid Mixed-Species CLT Panels with Sugar Maple and White Spruce. *Journal of Materials in Civil Engineering*, *33*(7), 04021171.

[14] Hematabadi, H., Madhoushi, M., Khazaeyan, A., & Ebrahimi, G. (2021). Structural performance of hybrid Poplar-Beech cross-laminated-timber (CLT). *Journal of Building Engineering*, 102959.

[15] Adnan, N. A., Tahir, P. M., Husain, H., Lee, S. H., Uyup, M. K. A., Arip, M. N. M., & Ashaari, Z. (2021). Effect of ACQ treatment on surface quality and bonding performance of four Malaysian hardwoods and cross laminated timber (CLT). *European Journal of Wood and Wood Products*, *79*(2), 285-299.

[16] Ukyo, S., Miyatake, A., Shindo, K., & Hiramatsu, Y. (2021). Shear strength properties of hybrid (hinoki cypress and Japanese cedar) cross-laminated timber. *Journal of Wood Science*, *67*(1), 1-18.

[17] Kaboli, H. (2019). Northeastern Species in Hybrid Cross Laminated Timber. Doctoral dissertation, University of Massachusetts Amherst, USA

[18] Rahman, M. D., Ashraf, M., Ghabraie, K., & Subhani, M. (2020). Evaluating timoshenko method for analyzing CLT under out-of-plane loading. *Buildings*, 10(10), 184.

[19] Li, X., Ashraf, M., Subhani, M., Kremer, P., Kafle, B., & Ghabraie, K. (2020). Experimental and numerical study on bending properties of heterogeneous lamella layups in cross laminated timber using Australian Radiata Pine. Construction and building materials, 247, 118525.

[20] Wang, Z., Fu, H., Gong, M., Luo, J., Dong, W., Wang, T., & Chui, Y. H. (2017). Planar shear and bending properties of hybrid CLT fabricated with lumber and LVL. *Construction and Building Materials*, *151*, 172-177.

[21] Larkin, B. 2017. Effective bonding parameters for hybrid cross-laminated timber (CLT). M.Sc. dissertation, Oregon State University, USA.

[22] Wei, P., Wang, B. J., Wang, L., Wang, Y., Yang, G., & Liu, J. (2019). An exploratory study of composite cross-laminated timber (CCLT) made from bamboo and hemlock-fir mix. *BioResources*, *14*(1), 2160-2170.

[23] Li, Q., Wang, Z., Liang, Z., Li, L., Gong, M., & Zhou, J. (2020). Shear properties of hybrid CLT fabricated with lumber and OSB. *Construction and Building Materials*, *261*, 120504.

[24] Cherry, R., Manalo, A., Karunasena, W., & Stringer, G. (2019). Out-of-grade sawn pine: A state-of-the-art review on challenges and new opportunities in cross laminated timber (CLT). *Construction and Building Materials*, 211, 858-868

[25] Dong, W., Wang, Z., Zhou, J., & Gong, M. (2021). Experimental study on bending properties of cross-laminated timber-bamboo composites. *Construction and Building Materials*, *300*, 124313.

[26] Wang, R., Shi, J. J., Xia, M. K., & Li, Z. (2021). Rolling shear performance of cross-laminated bamboo-balsa timber panels. *Construction and Building Materials*, *299*, 123973.

[27] Xu, B. H., Zhang, S. D., Zhao, Y. H., & Bouchaïr, A. (2021). Rolling shear properties of hybrid cross-laminated timber. *Journal of Materials in Civil Engineering*, 33(7), 04021159.

[28] Meethaworn, B., Srivaro, S., & Khongtong, S. (2020). A novel densifying method for the development of high strength rubberwood for structural application. *Construction and Building Materials*, 265, 120862.

[29] Srivaro, S., Tomad, J., Shi, J., & Cai, J. (2020). Characterization of coconut (Cocos nucifera) trunk's properties and evaluation of its suitability to be used as raw material for cross laminated timber production. *Construction and Building Materials*, 254, 119291.

[30] Prachasaree, W., Limkatanyu, S., & Yai, H. (2013). Performance evaluation of FRP reinforced Para wood glued laminated beams. *Wood Research*, 58(2), 251-264.

[31] Fathi, L. (2014). Structural and mechanical properties of the wood from coconut palms, oil palms and date palms. Doctoral dissertation, University of Hamburg, Germany.

[32] Yusoh, A. S., Tahir, P. M., Uyup, M. K. A., Lee, S. H., Husain, H., & Khaidzir, M. O. (2021). Effect of wood species, clamping pressure and glue spread rate on the bonding properties of cross-laminated timber (CLT) manufactured from tropical hardwoods. *Construction and Building Materials*, *273*, 121721.

[33] ASTM D 2395-17 (2017) Standard Test Methods for Density and Specific Gravity (Relative Density) of Wood and Wood-Based Materials. ASTM Annual Book of Standards. ASTM International, West Conshohoken.

[34] ASTM D 143 – 21 (2021) Standard Test Method for Small Clear Specimens of Timber. ASTM Annual Book of Standards. ASTM International, West Conshohoken.

[35] Kretschmann, D.E. (2010). Mechanical properties of wood, in: R.J. Ross (Ed.), Wood Handbook: Wood as an Engineering Material, Forest Product Laboratory, Madison.

[36] ASTM D905 - 08(2021) Standard Test Method for Strength Properties of Adhesive Bonds in Shear by Compression Loading. ASTM Annual Book of Standards. ASTM International, West Conshohoken.

[37] Gibson, L. J. (2012). The hierarchical structure and mechanics of plant materials. *Journal of the royal society interface*, *9*(76), 2749-2766.

[38] Gibson, L.J., &Ashby, M.F. (1997) Cellular Solids: Structure and properties (Second Ed) Cambridge University Press, Cambridge.

[39] Borrega, M., & Gibson, L. J. (2015). Mechanics of balsa (Ochroma pyramidale) wood. *Mechanics of Materials*, 84, 75-90.

[40] He, M., Sun, X., Li, Z., & Feng, W. (2020). Bending, shear, and compressive properties of three-and five-layer cross-laminated timber fabricated with black spruce. Journal of Wood Science, 66(1), 1-17.

[41] He, M., Sun, X., & Li, Z. (2018). Bending and compressive properties of cross-laminated timber (CLT) panels made from Canadian hemlock. Construction and Building Materials, 185, 175-183.

[42] Cao, Y., Street, J., Li, M., & Lim, H. (2019). Evaluation of the effect of knots on rolling shear strength of cross laminated timber (CLT). Construction and Building Materials, 222, 579-587.

[43] Li, M., Dong, W., & Lim, H. (2019). Influence of lamination aspect ratios and test methods on rolling shear strength evaluation of cross-laminated timber. Journal of Materials in Civil Engineering, 31(12), 04019310.

[44] Li, M. (2017). Evaluating rolling shear strength properties of cross-laminated timber by short-span bending tests and modified planar shear tests. Journal of Wood Science, 63(4), 331-337.

[45] Meylan, B. A. (1978). Density variation within Cocos nucifera stems. New Zealand Journal of Forestry Science, 8(3), 369-383.